Materials Transactions, Vol. 43, No. 10 (2002) pp. 2443 to 2448
Special Issue on Superplasticity and Its Applications

Superplastic Forming of AZ31 Magnesium Alloy Sheet into a Rectangular Pan

Abdel-Wahab El-Morsy, Ken-ichi Manabe and Hisashi Nishimura

Department of Mechanical Engineering, Tokyo Metropolitan University, Tokyo 192-0397, Japan

Superplastic behaviour of Mg-alloy AZ31 was investigated to clarify the possibility of its use for superplastic forming (SPF) and to accurately evaluate material characteristics under a biaxial stress by utilizing a multi-dome test. The material characteristics were evaluated under three different superplastic temperatures, 643, 673, and 703 K in order to determine the most suitable superplastic temperature. Finite Element Method (FEM) simulation of rectangular pan forming was carried out to predict the formability of the material into a complex shape. The superplastic material properties are used for the simulation of a rectangular pan. Finally, the simulation results are compared with the experimental results to determine the accuracy of the superplastic material characteristics. The experimental results revealed that the *m* values are greater than 0.3 under the three superplastic temperatures, which is indicative of superplasticity. The optimum superplastic temperature is 673 K, at which a maximum *m* value and no grain growth were observed. The results of the FEM simulation revealed that certain localized thinning occurred at the die entrance of the deformed rectangular pan due to the insufficient ductility of the material. The simulation results also showed that the optimum superplastic temperature of AZ31 is 673 K.

(Received April 22, 2002; Accepted July 10, 2002)

Keywords: *superplasticity, Mg-alloy, material testing, multi-dome test, blow forming, rectangular pan, finite element method*

1. Introduction

Recently, there has been a great interest in using lightweight materials for automotive[1–7] and aerospace components.[1–3] Magnesium is expected to become the best alternative material for lightweight components due to its low density. Magnesium offers several advantages: low density (1.74 g/cm^3),[8] outstanding damping capacity,[9] dimensional stability,[5] and high specific strength and stiffness.[1,10] In addition to these basic characteristics, its high recyclability at low energy cost is favored to significantly reduce environmental pollution.[1,11] However, the usage of magnesium alloy in more complexly shaped products is limited by insufficient ductility. Superplastic forming (SPF) is a viable technique that can be used to form magnesium into complex shapes. Until now, only limited knowledge has been available about the superplastic behaviour of Mg alloys.

In this work, superplastic behavior of Mg-alloy AZ31 was investigated to explore the possibility of its use for SPF and to evaluate accurate material characteristics under a biaxial stress by utilizing a multi-dome test. The experiments were conducted at three different superplastic (SP) temperatures 643, 673, and 703 K in order to determine the most appropriate SP temperature for the material. Models of rectangular pan forming were carried out to predict the formability of the material into a complex shape and to determine the most appropriate superplastic temperature. Finally, the simulation results are compared with the experimental results to determine the accuracy of the material characteristics.

2. Material Testing

The interdependence of SP material testing and process modelling is essential for optimizing the SPF. The testing method most widely used for material property determination is the tensile test. However, a major limitation of this material testing is a lack of accuracy of material characteristics. It describes the variation in flow stress with the strain rate that occurs during the forming into complex parts. This inaccuracy comes from the uniaxial loading in the tensile testing methods, which does not reflect accurately the stress state in the SP forming process. In actual SPF, the material is stretched under biaxial stresses. Simulation of SPF dependening on uniaxial SP material properties may lead to inaccuracy in the final product.

The authors developed a new testing method "Multi-dome test" to evaluate the SP material characteristics under a biaxial stress, which represents the state of the actual forming process.[12,13] In this testing method, SP material characteristics were determined by the following equations:

$$\sigma_{\mathrm{e}} = K\dot{\varepsilon}_e^{\mathrm{m}} \tag{1}$$

$$\sigma_{\mathrm{e}} = \frac{pr}{2t_{\mathrm{f}}} = \frac{p}{4t_{\mathrm{f}}}\left(\frac{h^2+R^2}{h}\right) \tag{2}$$

$$\varepsilon_{\mathrm{e}} = \left|\ln\frac{t_{\mathrm{f}}}{t_{\mathrm{i}}}\right| \tag{3}$$

$$m = \frac{d\log\sigma}{d\log\dot{\varepsilon}} = \frac{\log(\sigma_2/\sigma_1)}{\log(\varepsilon_2/\varepsilon_1)} = \frac{\log(\sigma_{\mathrm{e}2}/\sigma_{\mathrm{e}1})}{\log(\varepsilon_{\mathrm{e}2}/\varepsilon_{\mathrm{e}1})} \tag{4}$$

where σ_{e} is the effective flow stress, K is the strength coefficient, m is the strain rate sensitivity index, $\dot{\varepsilon}_{\mathrm{e}}$ is the effective strain rate, p is the forming pressure, t_{f} is the final thickness, t_{i} is the initial thickness, h is the bulging height, and R is the radius of the die cavity.

The material used in this study was Mg-alloy AZ31 1 mm in thickness. The chemical composition of the material is shown in Table 1. For the investigation of the most suitable SP temperature, three different temperatures of 643, 673, and 703 K were chosen.

Table 1 Chemical composition of AZ31 (Unit: [%]).

Al	Zn	Mn	Si	Cu	Ni	Mg
2.9	1.1	0.49	1.0	0.1	0.03	Balance

3. Finite-Element Simulation

Finite-element (FE) simulation was carried out for SP rectangular pan forming. The rectangular pan provides a plane-strain section at the centre of the long side, and areas of biaxial straining at the corners. The die used to form the trays has a rectangular cavity 80 mm wide, 120 mm long and 20 mm deep. A die entrance radius of 1 mm enables the transition from the flat rim 8 mm in width to the rectangular cavity as shown in Fig. 1. The FE code used is the MARC. In this model, a FE mesh was generated using 4-node 3D-shell elements.

In this work, the rigid plastic flow (RP-Flow) formulation was used to simulate SP rectangular pan forming. RP-Flow is appropriate for analysis of SP metal forming since the initial yield strength is low and plastic strains are typically orders of magnitude greater than the elastic strains. The material characteristics, obtained by the multi-dome forming test, were applied in the simulation through the subroutine programmed in the solver. The subroutine enables easy definition of the equivalent stress as a function of equivalent strain rate, and it allows access to user-defined state variables that can be used to follow parameters such as strain rate sensitivity index, m, and strength coefficient, K. Coulomb's friction law with a constant die friction coefficient of 0.1 was used in the simulation.

Figure 2 shows the flow chart of the FE simulation process. The material parameters m and K were applied in the simulation as a function of strain rate. In our previous work,[14] the effect of the variation of material characteristics m and K on the deformation profile was investigated. The results showed that in order to anticipate correct analytical results it is necessary to take into account the variation in m and K values with various strain rates. Figure 3 shows the flow chart of the subroutine and the main program used in the work. In FE simulation, the relationship between the flow stress and the strain rate is defined by the constitutive equation without considering the grain growth or the strain hardening [eq. (1)].

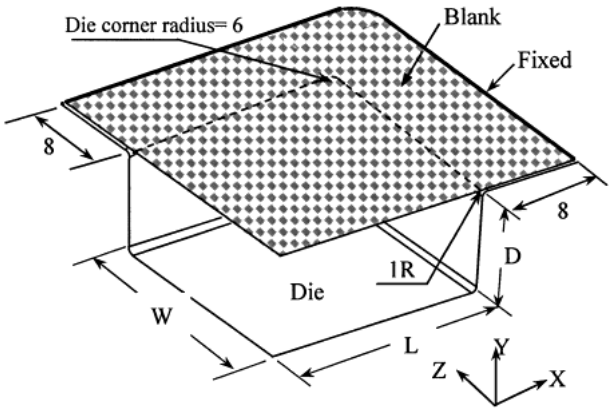

Fig. 1 Illustration of FE model of rectangular pan and boundary conditions of blank.

4. Results and Discussion

4.1 Experiments of multi-dome testing method

4.1.1 SP material characteristics

The greatest advantage of the evaluation by the multi-dome test is the capacity to evaluate characteristics simultaneously

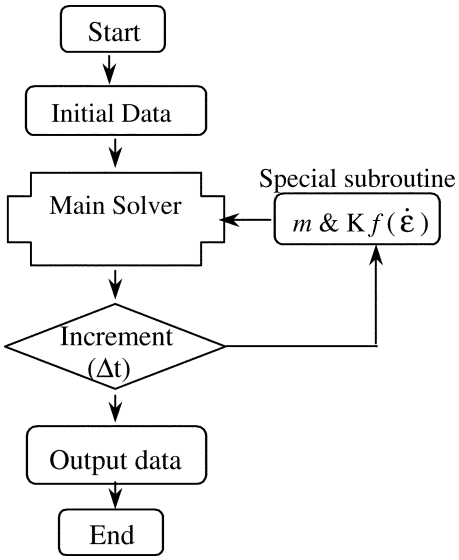

Fig. 3 Flow chart of subroutines and main program.

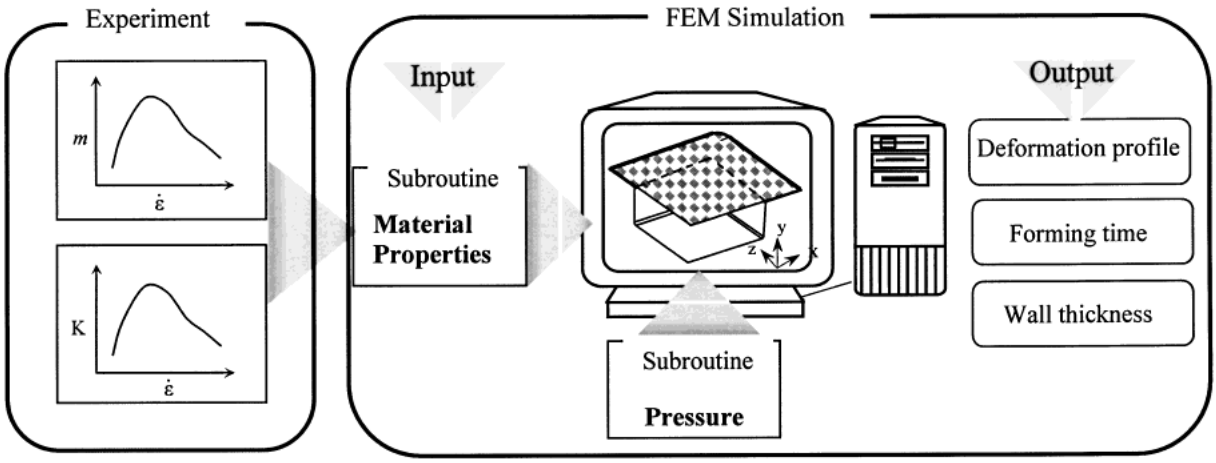

Fig. 2 Flow chart of FE simulation of rectangular pan.

at different strain rates. It is a notable merit that the data for the extended range of the strain rate can be obtained from a single sheet of metal, through the strain rates and the stresses at the dome apex for the four domes.

Figure 4 shows the relationship between the flow stress and the strain rates at different SP temperatures, 643, 673, and 703 K. The flow stress and strain rate values at the apex of the dome were obtained from the above-mentioned dome-forming equations [eqs. (1), (2), (3) and (4)]. Five experiments with different forming pressures and different bulge times (Table 2) were sufficient to obtain the curve with the strain rate ranging between 4×10^{-5} and $2 \times 10^{-3}\,s^{-1}$. These data sets were plotted together and then a curve was fitted by using the regression analysis to provide smoothed stress-strain rate relations. Increasing the temperature leads to a decrease in the flow stress. However, such temperature dependence is observed only in the range corresponding to a stable microcrystalline structure. If significant grain growth occurs with increasing temperature, the effect of superplasticity decreases abruptly or disappears completely.

Figure 5 shows the relationship between the strain rate and the strain rate sensitivity index, m. The m values were obtained by using the strain ratio between two domes (D1, D2, D3 and D4). It can be seen from this figure that at all the temperatures, maximum m values are over 0.3, which is indicative of superplasticity. The strain-rate range of superplasticity is small in the case of 643 K and wide in the case of 673 K. It is also evident that the maximum m value obtained at SP temperature 673 K is higher than those obtained at the other two temperatures, 703 and 643 K.

4.1.2 Microstructural observations

Figure 6 shows the microstructures of the Mg alloy after the multi-dome forming tests at three different SP temperatures compared with the original specimen before the test. The three experiments were conducted at the same forming pressure and the same bulge time. There is no difference in the grain size of the specimens deformed at 673 and 643 K, whereas, grain growth occurred in the specimen deformed at 703 K due to higher temperature. It is well known that grain size strongly influences the superplasticity of the materials; an increase of the grain size leads to a reduction in the maximum strain-rate sensitivity index, m.[15,16] A microstructural feature of the specimen at 703 K also shows that twins occurred in the specimen due to the effect of the grain growth (annealing twins),[17,18] which happened in the specimen at the elevated temperature. In contrast to the effect of the grain growth increasing the flow stress,[15] the effects of temperature and the twins decrease flow stress.

The results of the SP material characteristics and the microstructural observations show that the optimum SP temperature of Mg-alloy AZ31 is 673 K, at which a high m value in a wide range of strain rate was observed.

4.2 Simulation of rectangular pan forming

In order to verify the optimum SP temperature of AZ31, the rectangular pan forming process was simulated with material characteristics obtained at the three different temperatures, 643, 673 and 703 K.

4.2.1 Bulge time

Figure 7 shows the effect of the SP temperature on the estimated relative bulge time (simulation/experiment) of the rectangular pan. The estimated relative bulge time is also compared with the actual forming time that was measured in the experiment. The experiment of rectangular pan forming was

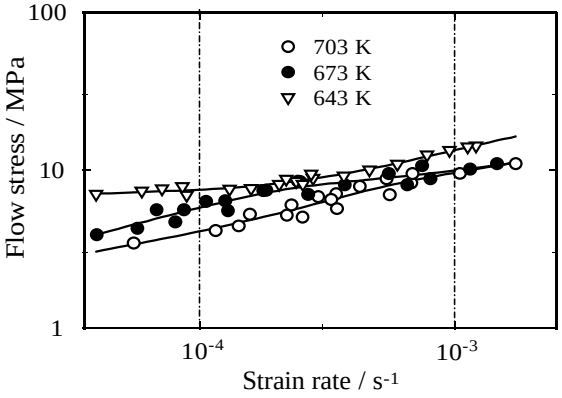

Fig. 4 Flow stress vs. strain rate relationship of AZ31.

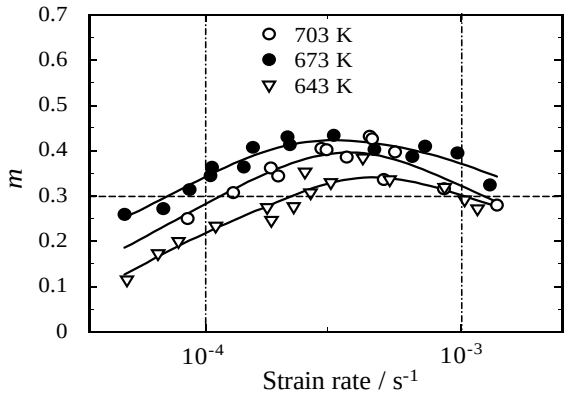

Fig. 5 Strain rate vs. strain rate sensitivity index m of AZ31.

Table 2 Experimental conditions of multi-dome test at three different SP temperatures.

No.	643 K		673 K		703 K	
	Forming pressure /MPa	Forming time /s	Forming pressure /MPa	Forming time /s	Forming pressure /MPa	Forming time /s
1	0.4	1200	0.4	1800	0.4	1800
2	0.6	1200	0.7	1800	0.7	1800
3	0.7	1500	0.7	2700	0.7	1200
4	0.9	900	0.9	1000	0.9	1000
5	0.9	300	0.9	300	0.9	450

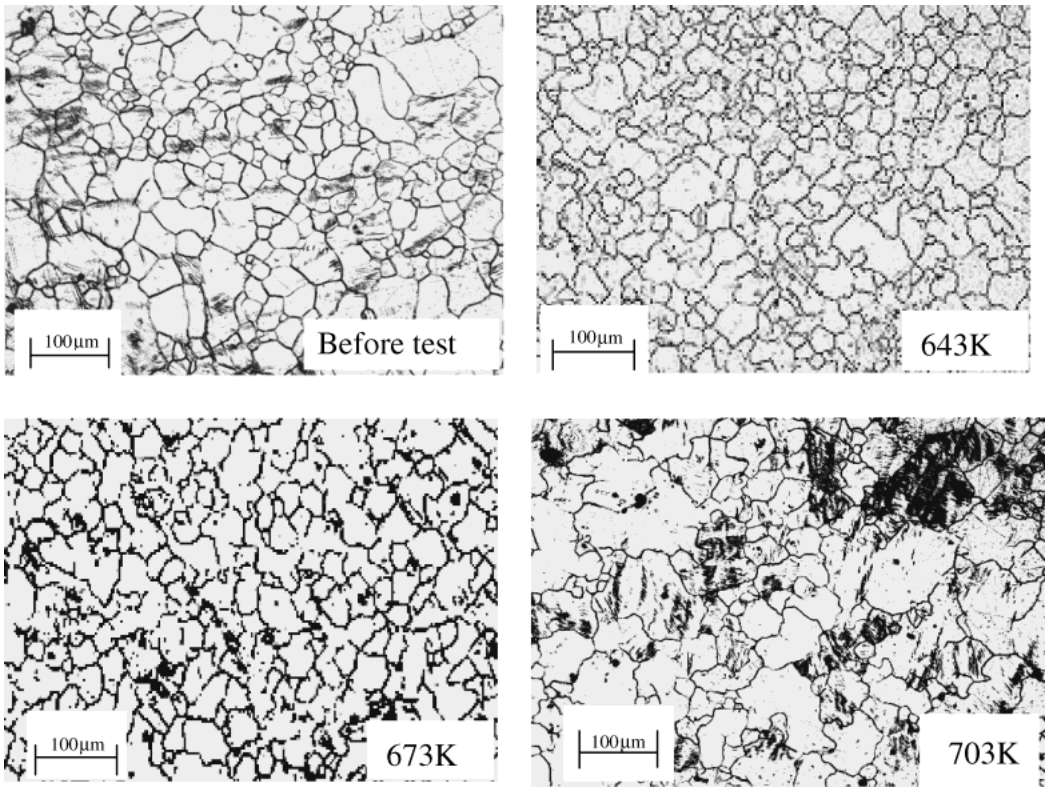

Fig. 6 Microstructures of the Mg-alloy specimens after the multi-dome tests at three different superplastic temperatures compared with the original specimen before the test.

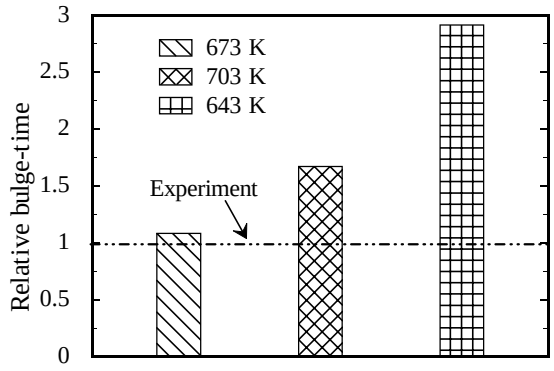

Fig. 7 Comparison of estimated bulge time and the actual experimental time.

performed using the same Mg-alloy sheet "AZ31" and was conducted at the SP temperature 673 K. The figure shows that the estimated bulge time with material characteristics obtained at SP temperature 673 K is very close to the measured bulge time of the experiment whereas, there is a notable difference in bulge time between estimated values and experimental ones, at 703 and 643 K for the formation of the rectangular pan. The great difference in bulge time between cases of SP temperatures 703 and 643 K is due to the effect of the *m* value as shown in Fig. 5, which has a strong influence on the estimation of the bulge time.[12,19,20] The accuracy of the estimated bulge time is decreased with a decreasing *m* value. The error in the estimated bulge time for the material characteristics at 673 K is less than 10%, whereas the error in the estimated bulge time in the case of 703 K is more than 60%. It exceeds 190% in the case of 643 K.

4.2.2 Wall thickness distribution

Figure 8 shows the comparison between the thickness profile of the completely formed pan with the predicted thickness at the centre cross section of the pan. From these figures, it is obvious that the thickness distribution of the deformed pan estimated by material characteristics obtained at 673 K is closer to the actual measured thickness of the experiment than those in cases of 703 and 643 K. There is a certain difference between the predicted thicknesses and the measured one. This is because the friction coefficient is assumed to be 0.1 in the simulation, whereas in the rectangular pan experiment, boron nitride was used as lubricant to reduce the friction between the sheet and the die.

These figures also show that localized thinning occurred at the die entrance in the formed rectangular pan. The localized thinning is due to (1) the effect of the die entry radius, which was 1 mm in the FE simulation of the pan, (2) the friction between the sheet and die surface and (3) the insufficient ductility of the material. Particularly, the material does not possess its full extent of softening at large strains. The localized thinning is more progressive in the transverse direction because the strain state of the pan is varied toward a plane strain condition. Thinning in the die entrance may not be accurate due to the fact that we did not consider bending strains because membrane elements were used in the model and localized thinning was often observed in this region.

Figure 9 shows the graphical output of FEM simulation of the deformed pan. This figure shows that a decrease in thickness of the deformed pan at the die entrance is greater in a transverse direction than in a longitudinal direction.

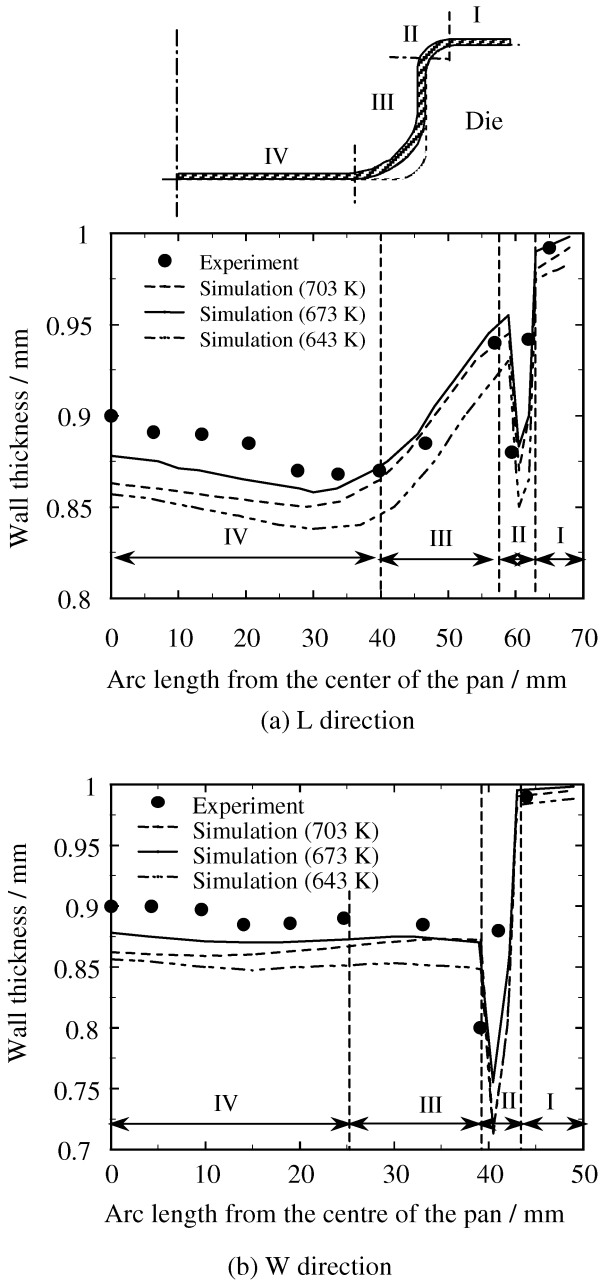

Fig. 8 Comparison of measured and predicted wall thickness at the centre cross section of the pan.

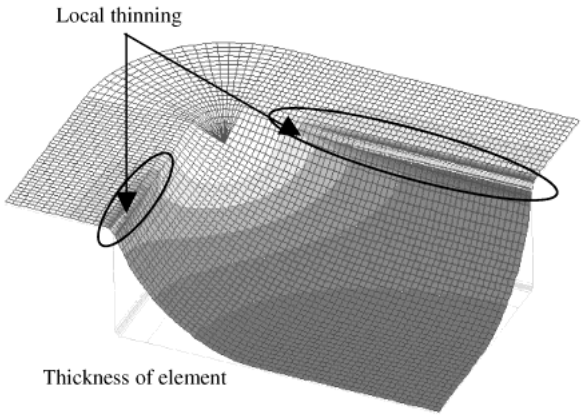

Fig. 9 Graphical output of FEM simulation of pan.

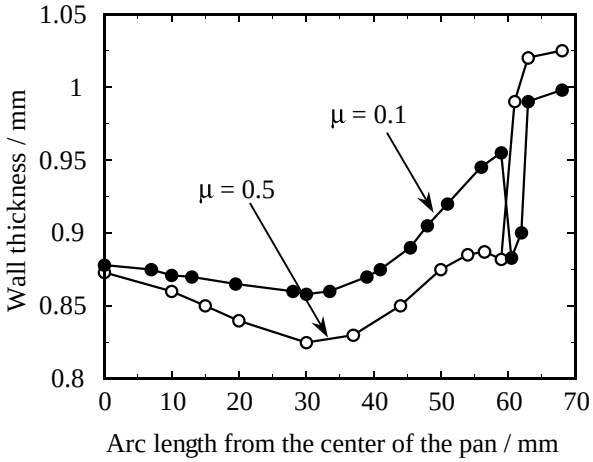

Fig. 10 Effect of friction coefficient on the predicted thickness distribution of deformed pan.

Figure 10 shows the effect of the friction coefficient on the predicted thickness distribution of deformed pan. It can be seen that the wall thickness shifts downward with increasing friction coefficient, because the frictional force decreases the volume flowing into the die cavity, and accordingly, the wall thickness distribution decreases. The localized thinning is seen to reduce with increasing friction coefficient.

5. Conclusion

In this work, SP behaviour of the Mg alloy AZ31 was investigated to clarify its ability of SPF and to evaluate accurate material characteristics under biaxial stress by utilizing a multi-dome test. The results of the multi-dome test revealed that AZ31 has potential for superplastic forming (m values are greater than 0.3) and the most appropriate SP temperature at which the highest m values are observed is 673 K ($m = 0.45$). There is no difference in grain size between the specimens deformed at 673 and 643 K. However, grain growth and annealing twins occurs in the specimen deformed at 703 K.

Rectangular box forming was simulated by FEM to predict the formability of the material into a complex shape and the appropriate SP forming temperature. The results show that the predicted bulge time and wall thickness distribution of the deformed rectangular pan estimated by material characteristics obtained at SP temperature 673 K are roughly in agreement with experimental ones. Localized thinning occurs at the die entrance of the deformed pan and exhibits a tendency to deform uniformly with increasing friction coefficient.

Acknowledgements

The authors wish to thank Dr. Koji KAKEHI and Mr. Nobuhisa KOISO of Tokyo Metropolitan University for their help in observing the microstructure.

REFERENCES

1) H. Furuya, N. Kogiso, S. Matunaga and K. Senda: Mater. Sci. Forum

350–351 (2000) 341–348.
2) H. Somekawa, M. Kohzu, S. Tanabe and K. Higashi: Mater. Sci. Forum **350–351** (2000) 177–182.
3) T. Mukai, M. Yamanoi and K. Higashi: Mater. Sci. Forum **350–351** (2000) 97–102.
4) E. Aghion and B. Bronfin: Mater. Sci. Forum **350–351** (2000) 19–28.
5) H. Watanabe, H. Tsutsui, T. Mukai, K. Ishikawa, Y. Okanda, M. Kohzu and K. Higashi: Mater. Sci. Forum **350–351** (2000) 171–176.
6) T. Mukai, H. Watanabe and K. Higashi: Mater. Sci. Forum **350–351** (2000) 159–170.
7) H. Friedrich and S. Schumann: J. Mater. Proces. Techno. **117** (2001) 276–281.
8) E. Doege and K. Droder: J. Mater. Proces. Techno. **115** (2001) 14–19.
9) H. Haferkamp, M. Niemeyer, R. Boehm, U. Holzkamp, C. Jaschik and V. Kaese: Mater. Sci. Forum **350–351** (2000) 31–42.
10) W. J. Kim, S. W. Chung, C. S. Chung and D. Kum: Acta Mater. **49** (2001) 3337–3345.
11) Yo Kojima: Mater. Sci. Forum **350–351** (2000) 3–18.
12) A. El-Morsy, N. Akkus, K. Manabe and H. Nishimura: Mater. Trans. **42** (2001) 2332–2338.
13) A. El-Morsy, N. Akkus, K. Manabe and H. Nishimura: Mater. Sci. Forum **357–359** (2001) 587–592.
14) A. El-Morsy and K. Manabe: J. Mater. Proces. Techno. **125–126**, pp. 778–783.
15) A. K. Ghosh and C. H. Hamilton: Metall. Trans. A **13A** (1982) 733–743.
16) C. H. Hamilton: J. Superplasticity, (1985) 14.1–14.14.
17) W. F. Hosford: *The Mechanics of Crystals and Textured Polycrystals*, (Oxford Engineering Science Publications, 1993) pp. 163.
18) D. VanAken: "Engineering Concepts: Formation of Annealing Twins". http://www.industrialheating.com/CDA/ArticleInformation/features/BNP_Features_Item/0,2832,13963,00.html
19) N. Akkus, K. Manabe, M. Kawahara and H. Nishimura: J. JSTP **39**, No. 445 (1998) 137–142.
20) N. Akkus: "Modeling and Process Control of Superplastic Free Bulge Forming", Ph. D. thesis, Tokyo Metropolitan University, (1999).